The Journal of the Korean Society of Oceanography
Vol. 32, No. 1, pp. 17-27, March 1997

Estimation of the Residence Time for Renewal of the East Sea Intermediate Water using MICOM

YOUNG HO SEUNG AND KUK JIN KIM
Dept. of Oceanogr., Inha Univ.

Miami Isopycnic Coordinate Ocean Model is applied to the East Sea to estimate the renewal time of the upper Intermediate Water. The model gives about 10 years of renewal time. Extrapolating this result to the whole water mass below, including the upper Intermediate Water, leads to about 81.4 years of renewal time, which is quite comparable to that obtained by Kim and Kim (1997) based on the recent observations. Deep winter mixing occurs in the north of the basin. The areas of the largest water mass conversion, from the upper mixed to the intermediate below, are along the periphery of the deep mixing zone. Large portion of the renewed Intermediate Water then advects along the Korean and Japanese coasts. It is concluded that the high-oxygen content Intermediate Water found off the Korean coast (Kim and Chung, 1984) is in part locally formed but mostly advected from the deep mixing zone.

INTRODUCTION

A surface layer called the Tsushima Current Water (TCW) enters into the East Sea through the Korea Strait (Fig.1). A small portion of it flows along the Japanese coast due to the topographic control (Yoon, 1982b) and the rest flows northward along the Korean Coast, forming the East Korean Warm Current (EKWC). The EKWC separates from the coast near 38° N, then moves eastward toward the Tsugaru and Soya Straits, where it leaves the East Sea. North of the warm current region, a cold current called the North Korean Cold Current (NKCC) or the Liman Current (LC) flows southward along the western boundary and meets with the EKWC where the EKWC separates from the coast. Most of these schematic features are generally confirmed by numerical models (Yoon, 1982a and b; Seung and Kim, 1993; Seung and Yoon, 1995b). The separation of the EKWC and the formation of the NKCC may be controlled by the wind stress curl and the buoyancy flux (Seung, 1992).

Most of the East Sea basin is filled with a very deep, cold and nearly homogeneous water, called the Japan Sea Proper Water (JSPW). There have been many questions about the formation, renewal and circulation of the JSPW and many of them still remain unknown. Recent observations indicate that this water mass has contained also the salinity minimum layer which is then named deep Intermediate Water in distinction from the conventional upper Intermediate Water. According to these observations, the JSPW has not been renewed for a long time (Kim and Kim, 1997). The presence of oxygen-rich Intermediate Water (IW) in the upper part of the JSPW (Uda, 1934; Kim & Chung, 1984; Kim *et al.*, 1991), however, suggests that a part of the deep/intermediate water is still formed somewhere. In fact, there is a dep winter mixing observed in the northwestern part of the basin (Seung & Yoon,

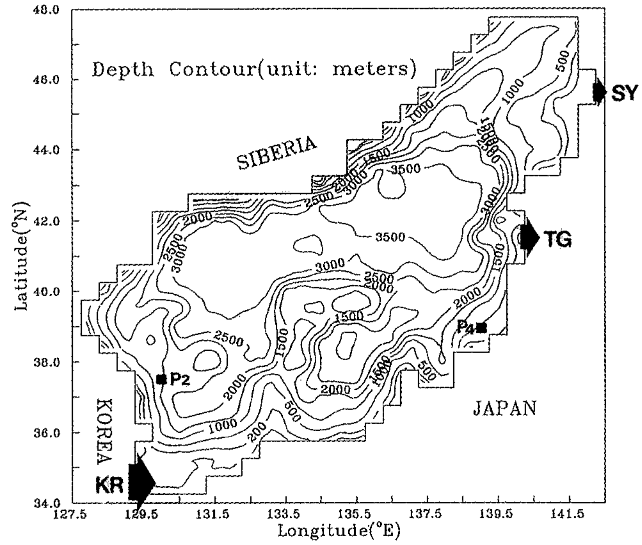

Fig. 1. Model domain with bottom topography. KR, TG and SY denote, respectively, Korea Strait, Tsugaru Strait and Soya Strait. P_2 and P_4 are locations where tracer concentrations are monitored.

1995a). Senjyu and Sudo (1994) also analysed the historical data to show that the upper portion of the JSPW extending over the whole basin originates from the northwest. They also suggested that the newly formed water mass circulates around the basin anti-clockwisely.

Numerical models have been used to study the deep circulation. Most of the models applied to the East Sea are of the Bryan-Cox type (Bryan, 1969; Cox, 1984), framed in the cartesian coordinates in the vertical, upon which the primitive equations for the fluid motion are discretised. Some layer models have also been used in modelling the whole (Sekine, 1986) or a part (Kawabe, 1982) of the basin. However, they were not able to handle the vanishing or outcropping of vertical layers, which is an essential feature for the regions of deep water formation like the one considered here. As noted in Seung and Kim (1993), a long-term drift of warming and thickening of deep layer is inevitable in these models due to the numerically induced diapycnal diffusion. The recently developed isopycnic coordinate ocean models such as the one considered here can handle these problems and are suitable in modeling the formation and circulation of the IW in the East Sea. This kind of model was first applied to the East Sea by Seung and Kim (1995). Their model has used simple dynamics with least dissipative effects, idealized wind and buoyance forcings, and idealized basin geometry. This model has successfully shown the outcropping and formation of the IW. The roles of three major forcings (inflow-outflow, wind and buoyancy) driving the circulation have been analysed in this study. The isopycnic coordinate model applied in present study (Bleck *et al.*, 1992) is much more advanced than the previous one (Seung and Kim, 1995) in that it uses complete equations, handles realistic bottom topography and deals with variable mixed layer depth as well as it allows surface and bottom outcroppings of isopycnic surfaces. As shown by Roberts *et al.* (1996), the advantages of the isopycnic coordinate models over those using cartesian vertical coordinate arise essentially from the facts that mixing of fluid is largely isopycnic and that the formers can cope with any depth without the need of transforming it onto a discrete set of depths.

As a first step to apply the Isopycnic Coordinate model to the East Sea, we estimate in this paper the time scale of renewal of the upper IW by using the Miami Isopycnic Coordinate Ocean Model (Bleck et al., 1992) with minimum resolution in both horizontal and vertical directions.

MODEL

The model is the same as that used by Bleck *et al.* (1992) except that inflow and outflow through open boundaries are added. The model allows the free surface and uses a mixed layer of the Kraus and Turner (1967) type with dissipation parameterized according to Gaspar (1988). It advances the barotropic and baroclinic solutions using a split-explicit scheme. The eddy viscosity used in isopycnal mixing of momentum depends on the horizontal shear, which is about 1,000 m^2/sec in this model. To handle the advection of sharp discontinuity of density interfaces, special schemes such as the Flux Corrected Transport (Zalesak, 1979) and the Multidimensional Positive Definite Advection Transport Algorithm (Smolarkiewicz, 1983 and 1984) are employed. For more details about the model, the reader is referred to Bleck *et al.* (1992).

The model domain (Fig. 1) is divided into horizontal grid of 0.5° by 0.5° in latitude and longitude. Vertically, it is consisted of 4 layers. The first layer (initial thickness 100 m) is the mixed layer which has variable temperature and salinity, and depth. The second layer (initial thickness 100 m) with density 26.0 in sigma-t represents the TCW proper. The third (density 27.20 and initial thickness 300 m) and the fourth (density 27.45) ones represent, respectively, the IW and the JSPW. In each layer below the mixed layer, the salinity and layer thickness are updated. The temperature is automatically determined using the equation of state from the updated salinity and the fixed density.

To impose the buoyancy forcing at the surface, the mixed layer temperature and salinity are relaxed to the measured surface temperature and salinity values (JODC, 1978) using the Newtonian damping-type restoring formula with the coefficient having time scale one day; for the coefficient having time scale 10 days, nearly the same patterns with relatively reduced intensity are obtained. The temperature and salinity data used above are the same as those in Seung and Kim (1993). Direct application of known heat and salt fluxes, if available, is preferred. However, the estimation of heat and salt fluxes are not yet considered to be quite certain. The basin is also forced by surface wind stress available from the daily atmospheric pressure charts (Na *et al.*,

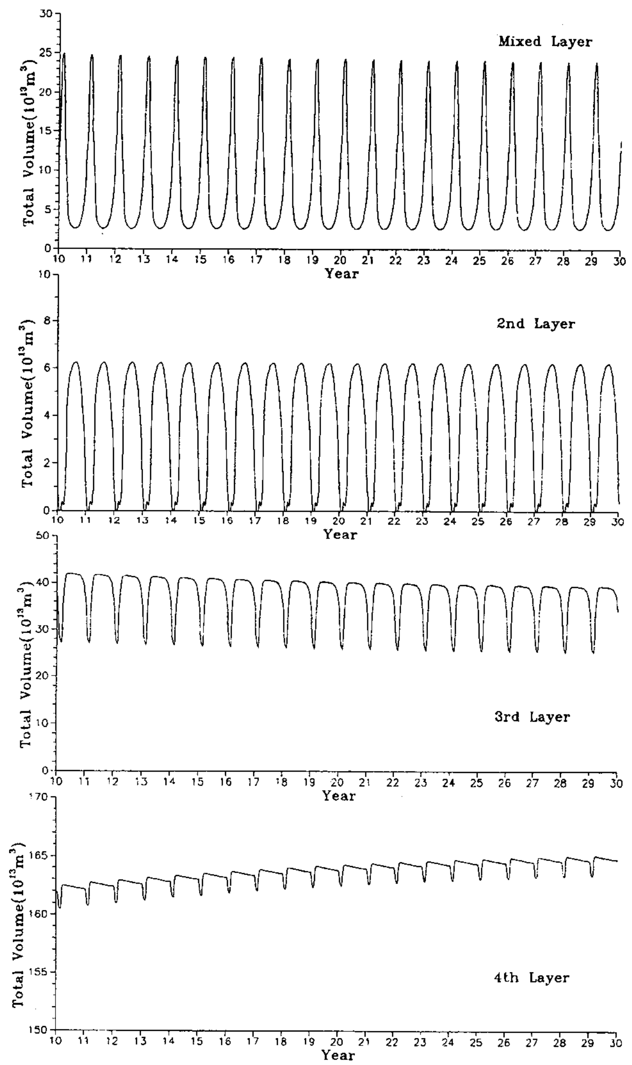

Fig. 2. Time series plots of the volume for each layer.

1992).

At the inflow opening (Korea Strait), a volume transport of 1.6 Sv is imposed through the mixed and second layers. Of this, 1.2 Sv flows out through the Tsugaru Strait and 0.4 Sv through the Soya Strait. Currents are assumed barotropic at the inlet and outlets. At the inflow opening, the mixed layer temperature, salinity and depth are also prescribed. The prescribed values are deduced from the observed ones (NFRDA, 1986) by assuming that the temperature and salinity of the inflowing second layer water (TCW) are constant. Instead, the temperature and salinity in the mixed layer are allowed to vary in such a way that the heat and salt within the water column are conserved. At the outflow openings, radiation boundary condition is applied for temperature, salinity and layer thickness.

Tracer experiment is performed by releasing the tracers in the mixed layer. The release is not confined within a particular area because the mixed layer is taken always saturated with the tracer. Vertical exchange of the tracer between the mixed and the layers below is determined by the mixed layer depth variation. In general, the tracers in layers below are lost to the mixed layer when the formers are engulfed by the latter during the winter convection but the formers gain more tracers from the latter when the mixed layer base retreats upward as spring heating progresses. The tracers left behind in the layers below are carried away by advection and diffusion within the layers. The isopycnal diffusion velocity is taken here as 1 cm, which corresponds to the usual diffusion coefficient of about 5×10^6 cm^2/sec in this model. The detrainment of the tracer from the mixed layer takes place either by the retreatment of the base of mixed layer or by the current crossing the interface.

RESULTS

The model was run for thirty years. Time series plots of the volume in each layer (Fig. 2) indicate large seasonal variations. The seasonal change occurs mostly in winter and becomes smaller for deeper layers. A quasi-steady state is reached after 30 years. The quasi-steady state is more evident in time series plots of the kinetic energy in each layer (Fig. 3). In winter, deep mixing reaches down to about 500 m (Fig. 4), which is somewhat less intense than, and which locates somewhat east of, the observed one (Seung and Yoon, 1995a). Current patterns in the mixed layer appear quite similar to those obtained in previous models (Fig. 5): in summer, the EKWC strengthens and extends northward. In winter, it weakens and retreats southward whereas the NKCC or the LC, flowing southward along the Siberian/Korean coast, develops and reaches far southward. This cold current has such a strong barotropic structure that it is found deep down to the bottom in January (Fig. 6). In February when the third layer is encroached upon by the mixed layer, currents follow largely the periphery of the deep mixing area (Fig. 7 and 8). However, there are components crossing the base of the mixed layer into the third layer especially near the coastal boundaries such as around 131° E, 41° N (Fig. 5 and 7). As explained later, this process may play an important role in the deep water formation. In

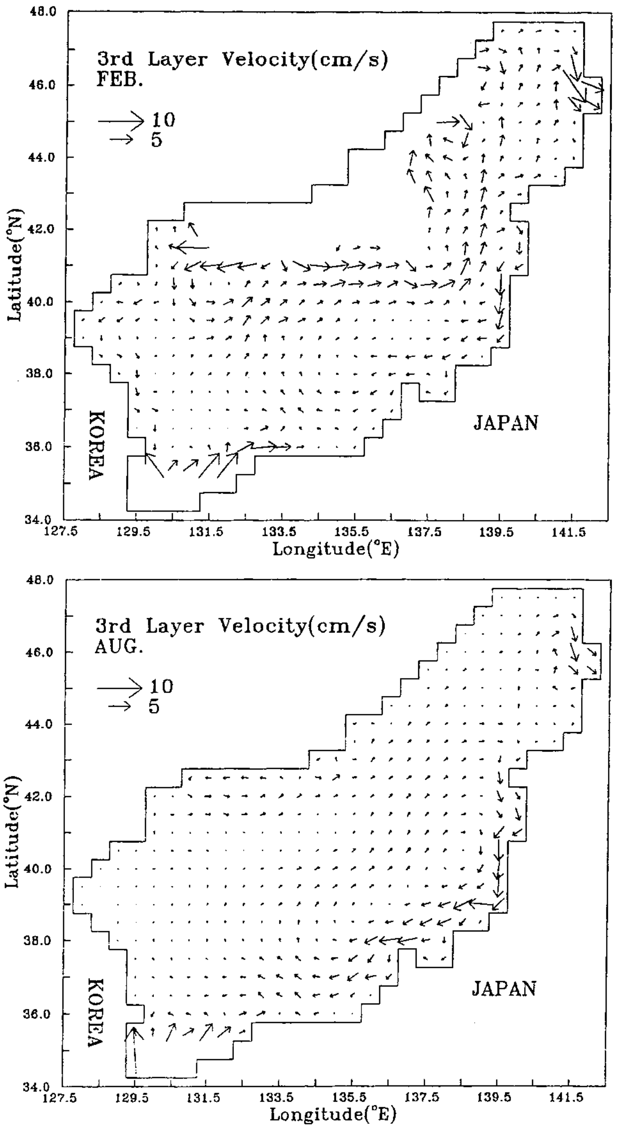

Fig. 7. Winter and summer distributions of the current in the third layer after 30 years of run.

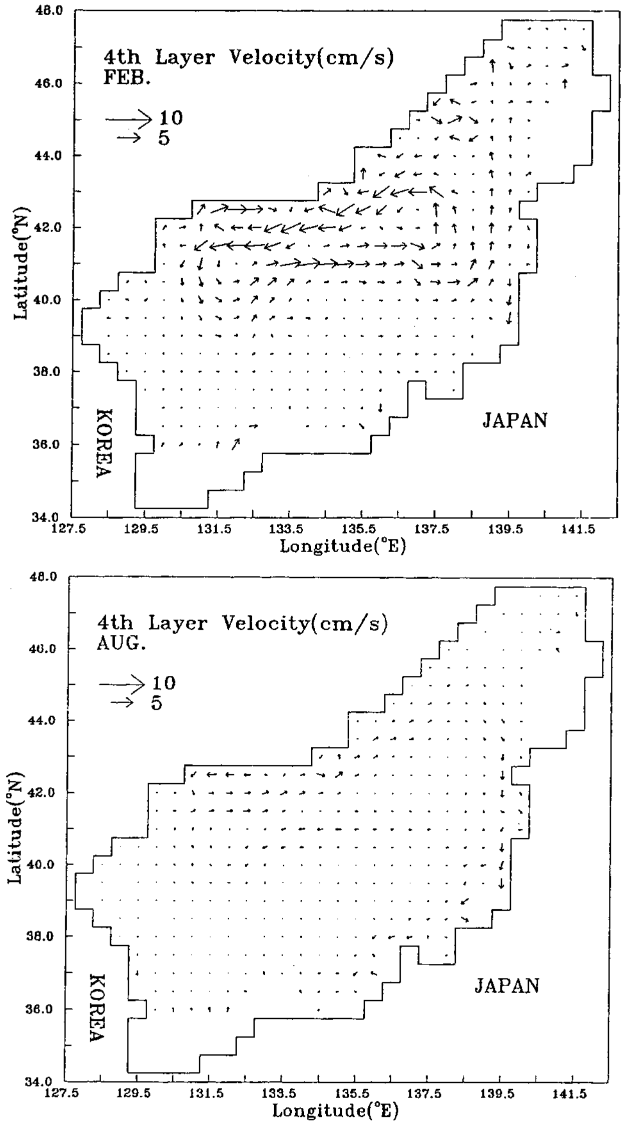

Fig. 8. Same as Fig. 7 except for the fourth layer.

tributed by each component is shown for the third (Fig. 16) and fourth (Fig. 17) layers. In the third layer, the most intense detrainment occurs around the periphery of the deep mixing zone although the detrainment with lesser degree of intensity is a ubiquitous feature over most of the basin. Referring to the current patterns in the mixed (Fig. 5) and in the third (Fig. 7) layers, a part of the detrainment occurring here may be due to the direct transport by horizontal current crossing the interface from the mixed to the third layers, as it is known for open oceans that most of the subduction into the lower layers occurs by lateral induction across the sloping base of the mixed layer rather than by the Ekman pumping alone (New *et al.*, 1995). The areas gaining the tracer by advection are the area inside the deep mixing zone and the area along Korean and Japanese coasts. It seems that the large amount of tracer detrained along the periphery of the mixing zone is carried into these areas. Large area just outside the deep mixing zone also loses the tracer by advection. The 4th layer gains most tracer inside the deep mixing zone by detrainment; outside it, the loss by entrainment to the upper layer is seen. The tracer inside the mixing zone is then advected horizontally outward. However, it does not take place along the coast as it does in the third layer.

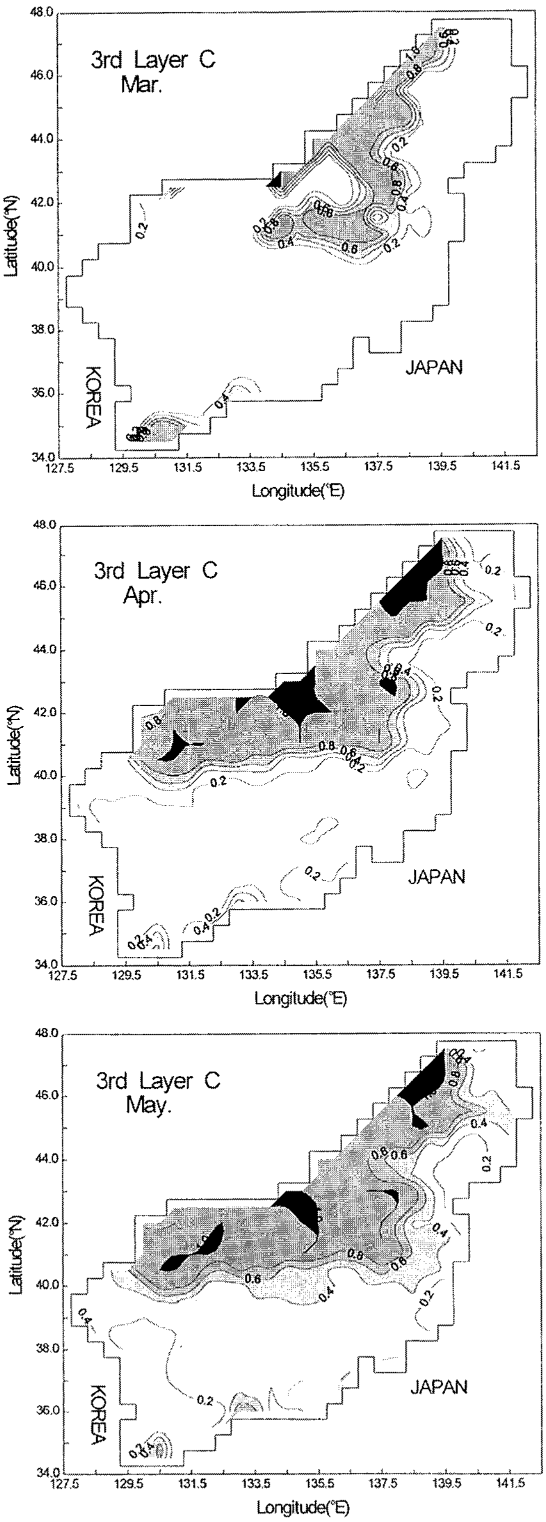

Fig. 9. Monthly change of concentration distributions in the third layer. Tracer is released on the first January of the same year.

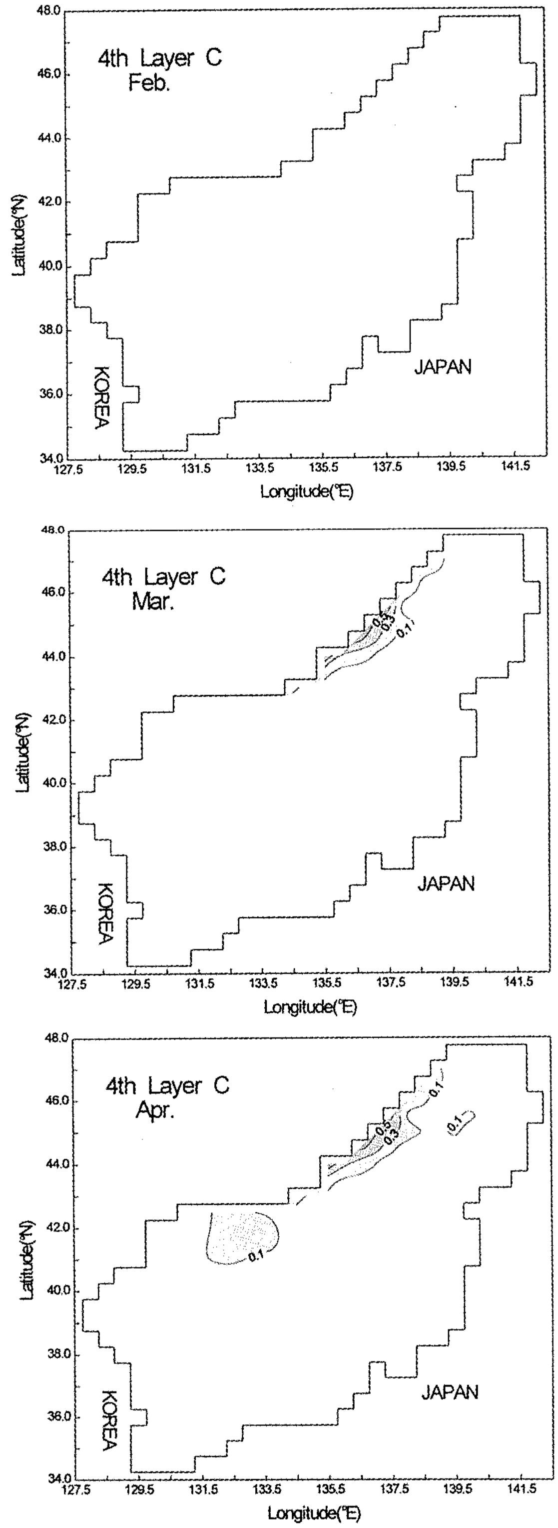

Fig. 10. Same as Fig. 9 except for the fourth layer.

CONCLUDING REMARKS

The results obtained in this model are not yet verified by observation. However, these results can be served as a guide to future investigations of the layers of IW and JSPW. They indicate that the residence time for renewal of IW is about ten years

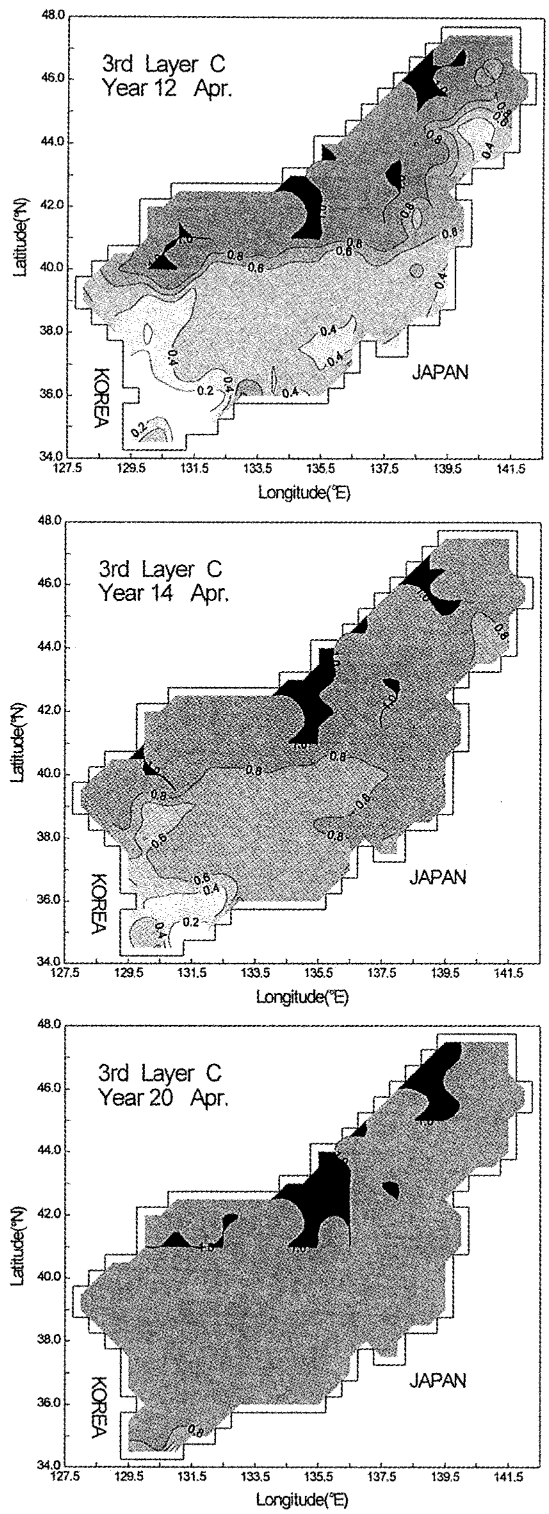

Fig. 11. Yearly change of concentration distributions in the third layer. Tracer is released at the beginning of year 11.

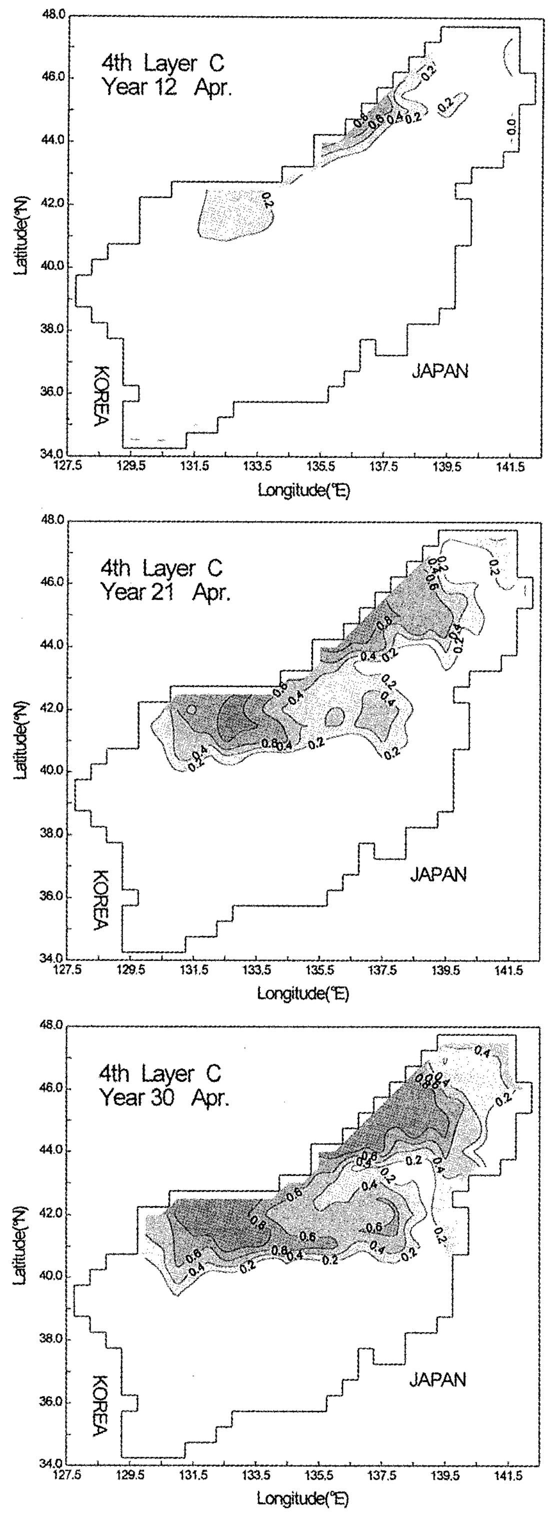

Fig. 12. Same as Fig.11 except for the fourth layer.

and much longer than 20 years for the JSPW. A rough estimation of the residence time for renewal of the whole third and fourth layers is possible because the tracer exchange for these layers as a whole occurs only through the upper boundary of the third layer. The third layer has thickness of about 350 m (superficial area of the basin is 1.16 ×

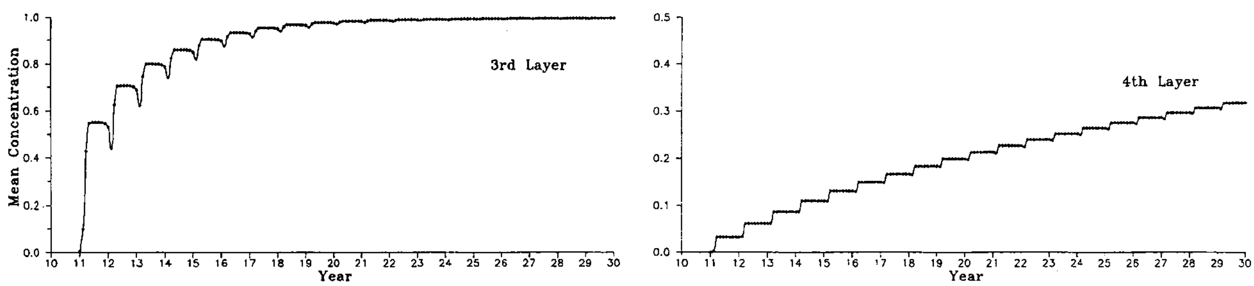

Fig. 13. Time series plots of the mean concentration over the third and fourth layers.

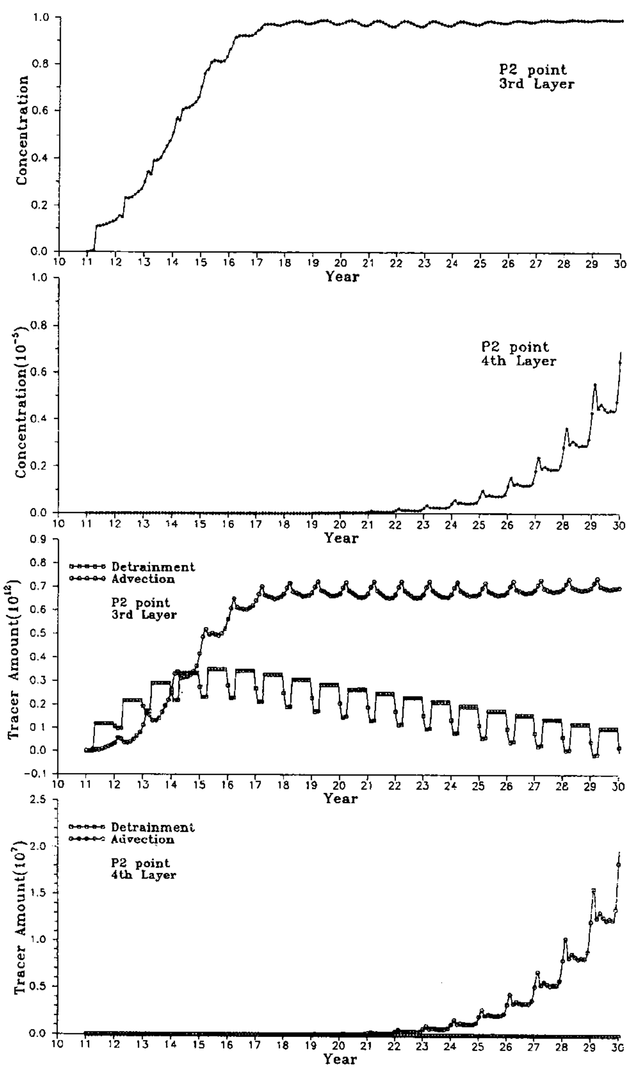

Fig. 14. Time series plots of the concentration in the third and the fourth layers at point P_2 (upper two panels). Time serieses of the tracer amounts due to the detrainment and the advection are also compared each other in each layer (lower two panels).

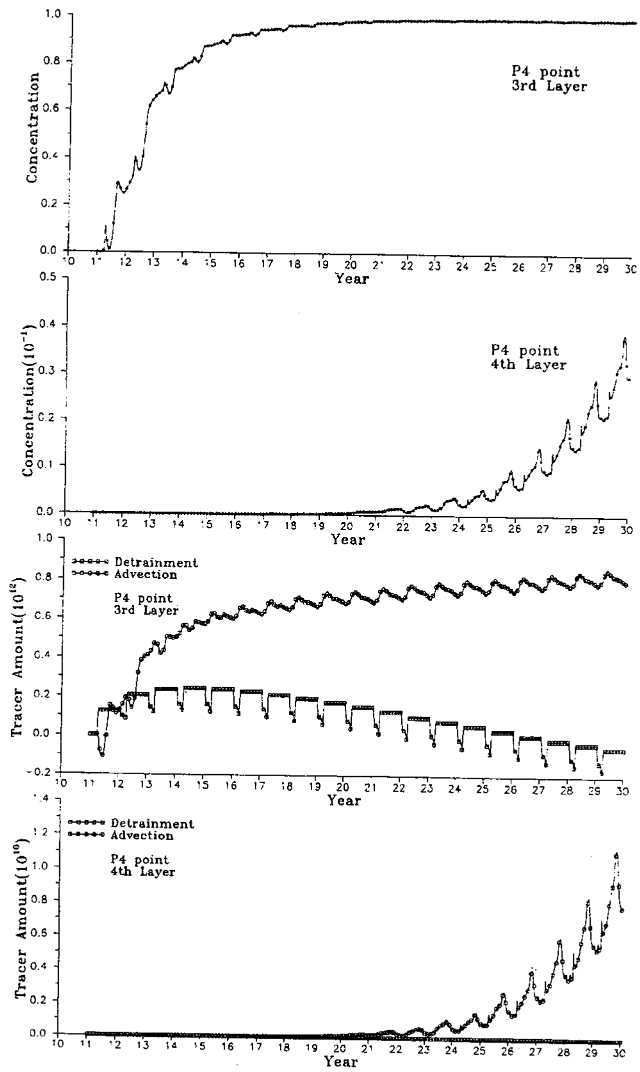

Fig. 15. Same as Fig. 14 except for at point P_4.

10^{12} m^2). The residence time is proportional to the total volume of the layer considered, which is about 2850 m multiplied by the superficial area in this case if the fourth layer thickness is taken as 2500 m. The residence time then becomes about 8.14 times that for the third layer alone, i.e., about 81.4 years, which is quite comparable to that obtained by Kim and Kim (1997) using a one dimensional model and observations. The renewal occurs through the detrainment from the mixed layer in winter. The

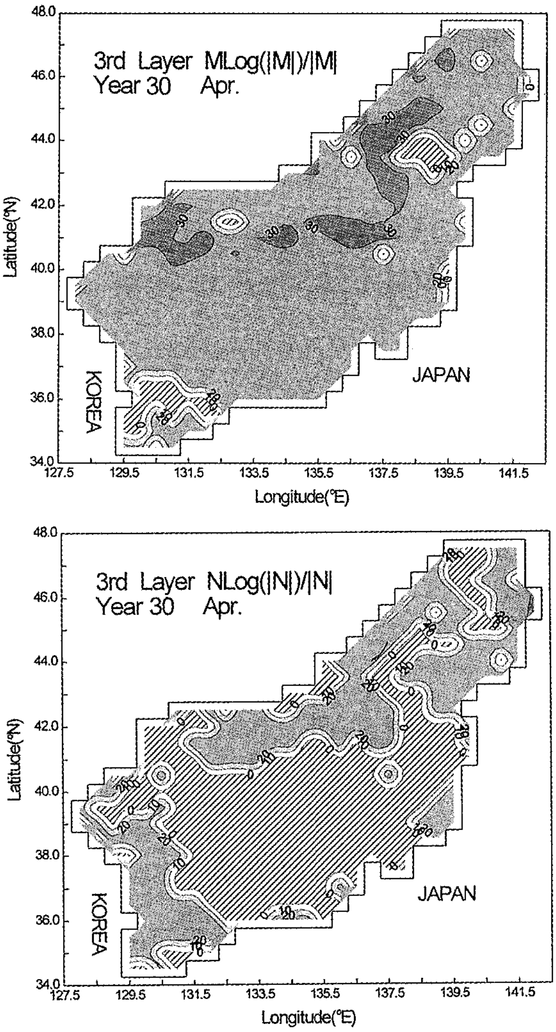

Fig. 16. Distributions of the tracer amounts due to the detrainment M and the advection N in the third layer in April. Values of M and N are log-scaled but their signs are retained. Areas with negative value are shaded with slanted lines. Tracer is released at the beginning of year 11.

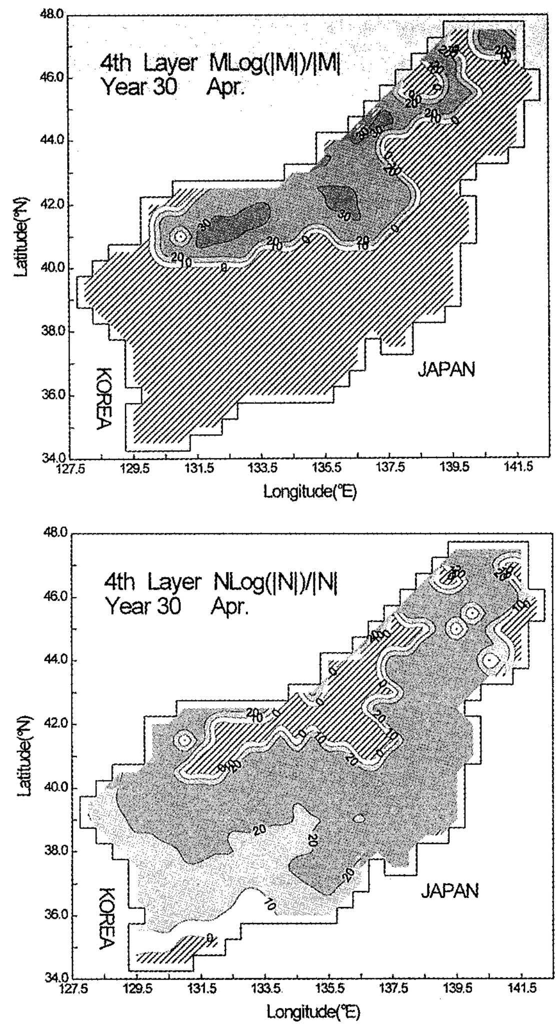

Fig. 17. Same as Fig.16 except for the fourth layer.

detrainment occurs over the large area of the basin but especially intensively around the periphery of the deep mixing zone, which forms in the northern part of the basin in winter. The newly formed IW is advected either to the inside of the mixing zone or to Korean and Japanese coastal regions. From the model results it seems that the IW of high oxygen content found off Korean coast (Kim and Chung, 1984) is in part locally formed but in most part advected from the area of intense formation. This advection seems to be carried out along Korean coast. Further detailed examination of the formation and circulation is possible only with higher resolution in both the horizontal and the vertical directions. This study will be done in near future.

ACKNOWLEDGEMENTS

This study is supported by NON DIRECTED RESEARCH FUND, Korea Research Foundation (1995~1998) and, in part, by Basic Science Research Institute Program, Ministry of Education (1996).

REFERENCES

Bleck, R., C. Rooth, D. Hu. and E.B. Kraus, 1992. Salinity-driven thermocline transients in a wind- and thermohaline-forced isopycnic coordinate model of the North Atlantic. *J. Phys. Oceanogr.*, **22**: 1486-1505.

Bryan, K., 1969. A numerical method for the study of the circulation of the world ocean. *J. Comput. Phys.*, **4**: 347-376.

Cox, M.D., 1984. A primitive Equation, 3-dimensional Model of the Ocean. Tech. Rep. No. 1, Ocean Group, GFDL, Princeton, 250 pp.

Gaspar, P., 1988. Modelling the seasonal cycle of the upper ocean. *J. Phys. Oceanogr.*, **18**: 161-180.

Japan Oceanographic Data Center, 1978. Marine Environmental Atlas, Northwestern Pacific Ocean I: Seasonal and Monthly, Japan Hydrographic Association.

Kawabe, M., 1982. Branching of the Tsushima Current in the Japan Sea. Part II. Numerical experiment. *J. Oceanogr. Soc. Japan*, **38**: 183-192.

Kim, C.H., H.J. Lie and K.S. Chu, 1991. On the intermediate water in the southwestern East Sea (Sea of Japan). In: Oceanography of Asian Marginal Seas, edited by K. Takano, Elsevier, Amsterdam.

Kim, K. and J.Y. Chung, 1984. On the salinity-minimum and dissolved oxygen-maximum layer in the East Sea (Sea of Japan). In: Ocean Hydrodynamics of the Japan and East China Seas, edited by T. Ichiye, Elsevier, Amsterdam.

Kim, K.-R. and Kuh Kim, 1997. What is happening in the East Sea (Japan Sea)?: Recent chemical observations during CREAMS 93-96. *J. Korean Soc. Oceanogr.* **31**(4): 164-172.

Kraus E.B. and J.S. Turner, 1967. A One-dimensional Model of the Seasonal Thermocline.

Na, J.Y., J.W. Seo and S.K. Han, 1992. Monthly-mean sea surface winds over the adjacent seas of the Korea Peninsular. *J. Oceanol. Soc. Korea*, **27**(1): 1-10.

National Fisheries Research and Development Agency, 1986. Mean Oceanographic Charts of the Adjacent Seas of Korea. Pusan, Korea. 186 pp.

New, A.L., R. Bleck, Y. Jia, R. Marsh, M. Huddleston and S. Barnard, 1995. An isopycnic model of the North Atlantic. Part I: Model experiment. *J. Phys. Oceanogr.*, **25**: 2667-2699.

Roberts, M., R. Marsh, A.L. New and R.A. Wood, 1996. An intercomparison of a Bryan- Cox type model and an Isopycnic ocean model. Part I: The subpolar gyre and high-latitude processes. *J. Phys. Oceanogr.*, **26**: 1495-1527.

Sekine, Y., 1986. Wind-driven circulation in the Japan Sea and its influence on the branching of the Tsushima Current. *Prog. Oceanogr.*, **17**: 297-312.

Senjyu, T. and H. Sudo, 1994. The upper portion of the Japan Sea proper water; Its source and circulation as deduced from isopycnal analysis. *J. Oceanogr.*, **50**: 663-690.

Seung, Y.H., 1992. A simple model for separation of East Korean Warm Current and formation of North Korean Cold Current. *J. Oceanol. Soc. Korea*, **27**(3): 189-196.

Seung, Y.H. and K. Kim, 1993. A numerical modeling of the East Sea circulation. *J. Oceanol. Soc. Korea*, **28**(4): 292-304.

Seung, Y.H. and J.H. Yoon, 1995a. Some features of winter convection in the Japan Sea. *J. Oceanogr.*, **51**: 61-73.

Seung, Y.H. and J.H. Yoon, 1995b. Robust diagnostic modeling of the Japan Sea circulation. *J. Oceanogr.* **51**: 421-440.

Seung, Y.H. and K.J. Kim, 1995. A multilayer model for dynamics of upper and intermediate layer circulation of the East Sea. *J. Oceanol. Soc. Korea*, **30**(3): 227-236.

Smolarkiewicz, P.K., 1983. A simple positive definite advection scheme with small implicit diffusion. *Mon. Wea. Rev.*, **111**: 479-486.

____, 1984. A fully multidimensional positive definite advective transport algorithm with small implicit diffusion. *J. Comput. Phys.*, **54**: 325-362.

Uda, M., 1934. Oceanographic conditions of the Japan Sea and its adjacent waters. *J. Imp. Fisher. Exp. St.*, **7**: 91-191. (in Japanese).

Yoon, J.H., 1982a. Numerical experiment on the circulation in the Japan Sea, Part I: formation of the East Korean Warm Current. *J. Oceanogr. Soc. Japan*, **38**: 43-51.

Yoon, J.H., 1982b. Numerical experiment on the circulation in the Japan Sea, Part III: mechanism of the Nearshore Branch of the Tsushima Current. *J. Oceanogr. Soc. Japan*, **38**: 125-130.

Zalesak, S.T., 1979. Fully multidimensional flux-corrected transport algorithms for fluids. *J. Comput. Phys.*, **31**: 335-362.